Heliyon 9 (2023) e21171

Contents lists available at ScienceDirect

Heliyon

journal homepage: www.cell.com/heliyon

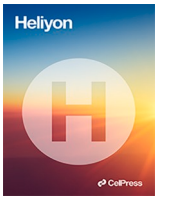

# Untargeted and spatial-resolved metabolomics characterize serum and tissue-specific metabolic reprogramming in acute kidney injury

Bei Xu [a,b,*], Wanyi Li [b], Yamei Zhang [b], Yan Chen [c], Jiafu Feng [b], Xiangrong Song [a,**]

[a] Department of Critical Care Medicine, Frontiers Science Center for Disease-related Molecular Network, State Key Laboratory of Biotherapy, West China Hospital, Sichuan University, Chengdu, Sichuan, China
[b] Department of Clinical Laboratory, Mianyang Central Hospital, School of Medicine, University of Electronic Science and Technology of China, Mianyang, Sichuan, China
[c] Department of Clinical Pharmacy, Sichuan Cancer Hospital & Institute, Sichuan Cancer Center, School of Medicine, University of Electronic Science and Technology of China, Chengdu, China

ARTICLE INFO

*Keywords:*
Untargeted metabolomics
Acute kidney injury
LC/MS
Spatial metabolomic analysis

ABSTRACT

*Background:* Acute kidney injury (AKI) is one of the most common clinical emergencies characterized by rapid progression, difficulty in early diagnosis, and high mortality. Currently, there are no effective AKI early diagnostic methods and treatments. Therefore, identifying new mechanisms of AKI have become urgent for development new targets for early diagnosis and treatment of AKI in the current clinical setting.

*Methods:* In this study, systematic analysis and comparison of serum metabolic profiles of clinical AKI patients, chronic kidney disease (CKD) patients, and healthy subjects were performed using untargeted metabolomics. Moreover, the first spatial metabolomic analysis of kidney tissues in an AKI mouse model using MALDI-TOF MS technology was conducted. Differentially expressed metabolites were identified using a comprehensive, publicly available database. The metabolic data obtained were evaluated using principal component analysis, (orthogonal) partial least squares discriminant analysis, and metabolic pathway analysis to explore the unique serum metabolic profile of the patients, as well as to characterize the spatial distribution of differential metabolites in the kidneys of AKI mice.

*Results:* Significant changes in the metabolite levels of amino acids, carnitine, and lipids were observed in the AKI and CKD groups versus the healthy population, suggesting that kidney injury may lead to abnormalities in various metabolic pathways, such as amino acids, fatty acids, and lipids. The significant difference between the AKI and CKD groups were found for the first time in these indexes including amino acid, carnitine, fatty acid, and lipid levels. Additionally, spatial metabolomics results revealed that amino acid, carnitine, organic acid, and fatty acid metabolites were more likely significantly altered in the renal cortex, while lipid metabolites were both differentially distributed in the cortex and medulla of the AKI group.

*Conclusion:* Abnormalities in the serum metabolism of amino acids, carnitine, and lipids in patients with kidney diseases, such as AKI and CKD, are closely associated with the physiological

* Corresponding author. Department of Critical Care Medicine, Frontiers Science Center for Disease-related Molecular Network, State Key Laboratory of Biotherapy, West China Hospital, Sichuan University, Chengdu, Sichuan, China.
** Corresponding author.
*E-mail addresses:* xb1990625@126.com (B. Xu), songxr@scu.edu.cn (X. Song).

https://doi.org/10.1016/j.heliyon.2023.e21171
Received 10 July 2023; Received in revised form 15 October 2023; Accepted 17 October 2023
Available online 1 November 2023

dysfunction of kidney injury. Metabolic differences between patients with AKI and CKD were compared for the first time, showing that fatty acid oxidative inhibition was more severe in patients with AKI. Furthermore, spatial metabolomics has revealed metabolic reprogramming with tissue heterogeneity in AKI mice model. Our study provides valuable information in the molecular pathological features of AKI in the kidney tissues.

## 1. Introduction

Acute kidney injury (AKI) is a common and critical clinical condition. Damage to kidney structure or function causes a rapid decline in renal function within 48 h [1]. Its clinical hallmarks include rapid progression, difficulty in early diagnosis, and high mortality rates [2]. Globally, AKI affects up to 10–15 % of hospitalized patients, and the incidence of acute kidney injury is as high as 60 % in critical care units [3]. Currently, AKI is primarily treated with symptomatic and supportive therapies as well as renal replacement; however, these have an extremely limited impact [4,5]. Thus, clarifying new mechanisms and providing new insights into the early diagnosis and treatment of AKI have become current clinical challenges.

Recently, a growing number of diseases have been linked to metabolic abnormalities, which are considered to contribute to the incidence and severity of a range of diseases, including cancer, and illnesses of the immune and inflammatory system [6]. The kidney is a highly metabolic organ [7] that regulates metabolite homeostasis and elevates the cellular metabolic status [7,8]. Previous studies confirmed that renal disease is closely associated with metabolic abnormalities. It not only promotes the development of renal disease but also leads to its progression [9,10]. Current studies on renal disease and metabolism have mainly focused on chronic kidney disease (CKD), and the findings include abnormalities in glucose, amino acid, and lipid metabolism [11–13]. Although studies targeting AKI metabolomics have already been performed in children born prematurely [14] or with renal transplantation [15], and in rat models of AKI induced by cisplatin [16], rhabdomyolysis [17], and sepsis [18], most clinical study samples were urine samples, and there are few systematic studies on changes in the serum metabolic profiles in adults with AKI. A 2012 pilot study showed elevated serum levels of acylcarnitine and amino acids (such as homocysteine, pyroglutamic acid, and dimethylarginine), and reduced levels of several lysophosphatidylcholines in 17 patients hospitalized for primary AKI, but the results require further validation in a larger sample of the AKI population [19].

AKI is increasingly being recognized as a major risk factor for CKD [20]. However, patients with AKI and CKD usually have similar clinical presentations, and some biological fluid markers diagnosing AKI, such as NGAL, KIM-1, IL-18, and L-FABP with suboptimal AKI diagnostic performance, also change significantly in CKD [21,22]. Thus, further research focusing on new specific biomarkers that can differentiate CKD from AKI is clinically important for the rapid identification and treatment of AKI and slowing down the progression of CKD. In addition, detailed knowledge of tissue-specific metabolic reprogramming of kidney injury is essential for a more accurate understanding of molecular pathological features and the development of novel therapeutic strategies. However, analysis of homogeneous biological samples such as urine, serum, and kidney homogenates using only HPLC-MS and NMR techniques provides little information on the spatial distribution of kidney metabolites. It is therefore necessary to use MS imaging-based spatial metabolomics, which can directly show the spatial distribution of metabolites in kidney tissue, thus enabling insight into biochemical changes associated with kidney injury within specific structures.

Therefore, this study systematically analyzed the metabolic profiles of serum from patients with clinical AKI using non-targeted metabolomics. We aimed to determine different in vivo metabolic mechanisms and find new biomarkers for the diagnosis of AKI. Furthermore, using MALDI-TOF MS technology, we performed a spatial metabolomic analysis of kidney tissues in a mouse model of AKI to investigate the spatial distribution characteristics of differential metabolites for the first time, further revealing metabolic reprogramming with tissue heterogeneity in AKI, and providing more comprehensive and detailed information on the molecular pathological characteristics of AKI kidney tissues.

## 2. Materials and methods

### 2.1. Study Design and participants

Between November 2020 and June 2022, 46 patients newly diagnosed with AKI and 65 patients with CKD participated in the study. Thirty-eight healthy volunteers without known chronic or major diseases and who were not undergoing any treatment were enrolled.

Inclusion criteria: 1) age $\geq$18 years; 2) acute kidney injury diagnosed according to the 2012 Kidney Disease Improving Global Outcomes (KDIGO) Clinical Practice Guideline for Acute Kidney Injury [23]. AKI is defined as any of the following: i) Increase in serum creatinine (sCr) $\geq$0.3 mg/dL ($\geq$26.5 μmol/L) within 48 h; ii) Increase in sCr $\geq$1.5 times of baseline within the prior 7 days; iii) Urine volume $<$0.5 mL/kg/h for 6h. 3) CKD was diagnosed according to 2012 KDIGO guidelines for CKD [24]. Patients with any of the following indicators lasting more than 3 months were diagnosed as CKD: i) urine albumin-to-creatinine ratio (UACR) $\geq$30 mg/g, ii) Abnormal urine sediment, such as visible white blood cells and red blood cells under the microscope, iii) Estimating Glomerular Filtration Rate (eGFR) $<$ 60 mL/min/1.73 $m^2$. CysC-based eGFR formula is used to calculate $eGFR_{CysC}$. The following formulas were

used for the calculations.

| | Serum cystatin C | Equation for estimating GFR |
|---|---|---|
| Female or male | ≤0.8 mg/l | $133 \times (SCysC/0.8)^{-0.499} \times 0.996^{Age}$ [ × 0.932 if female] |
| Female or male | >0.8 mg/l | $133 \times (SCysC/0.8)^{-1.328} \times 0.996^{Age}$ [ × 0.932 if female] |

This study excluded patients with symptoms of bacterial infection (such as fever, increased leukocyte and neutrophil counts, and inflammation) to avoid any influence of bacterial infection on the serum metabolome.

### 2.2. Sample Collection and preparation for serum non-targeted metabolomics

Fasting venous blood was taken after the patients were diagnosed and enrolled. Patients with AKI were generally drawn within 24–48 h after diagnosis, when most patients were in the extension and maintenance phase of AKI. Briefly, venous blood samples (5.0 mL each) were collected from all participants after overnight fasting. Serum was prepared by centrifugation at 3000 rpm for 10 min at room temperature, collected in 1.5-mL microfuge tubes, and stored at −80 °C until further analyses.

After thawing on ice, 100 μL of plasma was mixed with 300 μL of methanol: acetonitrile (1:1 v/v) solution to extract various small molecular metabolites. After vortexing, sonication, and incubation at −20 °C for 30 min, the supernatants were filtered and transferred to sample bottles with a 0.22-μm microporous membrane for further analysis. The same sample preparation methods were applied to the quality control (QC) samples, which were prepared by pooling aliquots of all serum samples (10 μL).

### 2.3. Serum metabolite Detection

An ultra-performance liquid chromatography (UPLC) system (Agilent 1290 Infinity II; Agilent Technologies Inc., CA, USA) connected to a high-resolution tandem mass spectrometer (TripleTOF 5600 Plus; AB SCIEX, Framingham, MA, USA) was used to conduct the metabolomic analysis. Previous methods of our lab were used for UPLC-MS/MS analysis [25]. Briefly, gradient chromatographic elution was performed on an ACQUITY HSS T3 column with the mobile phase composed of solvent A (water and 0.1 % formic acid) and solvent B (acetonitrile and 0.1 % formic acid). The mobile phase was delivered at a flow rate of 0.30 mL/min. The optimized electrospray ionization parameters were listed as follows: ion source gas 1, 55 psi; ion source gas 2, 55 psi; curtain gas, 35 psi; source temperature, 550 °C; declustering potential, 80 V; collision energy, 10 V; accumulation time: 0.15 s.

The mass accuracy was calibrated for every six samples throughout the study. Additionally, to evaluate the reliability of large-scale metabolomic analysis, QCs were introduced after every 10 samples.

### 2.4. Serum metabolomics analysis

Raw UPLC-MS/MS data were acquired and processed using Analyst TF software (version 1.7.1, AB SCIEX). As part of the metabolomic workflow, peaks were selected, their quality was assessed, and missing values were imputed, normalized, transformed, and scaled. The details are described in a previous study [25]. For accurate metabolite characterization, standard databases and custom databases including METLIN (http://metlin.scripps.edu/), Kyoto Encyclopedia of Genes and Genomes (KEGG) (http://www.kegg.jp/kegg/pathway.html), LipidMaps (https://www.lipidmaps.org/), Human Metabolome Database (HMDB) (https://hmdb.ca/), MassBank (https://massbank.eu/), and PubChem Database (https://pubchem.ncbi.nlm.nih.gov/) were used KEGG and MetaboAnalyst database exploration (http://www.metaboanalyst.ca/) were performed to identify enriched pathways based on altered metabolites.

### 2.5. Spatial metabolomics analysis of kidney of mouse model

A mouse model of AKI was established by using cisplatin to induce acute renal injury. An intraperitoneal injection of cisplatin (50 mg/kg, Sigma-Aldrich, St Louis, MO, USA) was administered to male C57BL/6 mice (weighing 20–25 g, aged 6–8 weeks). An equal volume of saline was administered to the control group. Mice were euthanized at 48 h after injection. Kidney tissues were obtained and snap frozen using liquid nitrogen and placed at −80 °C for use.

Using a Leica CM1950 cryostat (Leica Microsystems GmbH, Wetzlar, Germany), tissues were sectioned at 10-μm thickness at −20 °C. Subsequently, indium tin oxide (ITO)-coated electrically conductive slides were used to mount the tissue sections. The tissue sections were dried for 30 min in a vacuum desiccator. Desiccated tissue sections mounted on ITO glass slides were sprayed with 15 mg/mL DHB (2, 5-dihydroxybenzoic acid), dissolved in 90 %:10 % Acetonitrile: water using an HTX TM sprayer (Bruker Daltonics, Germany).

MALDI-TOF MSI experiments were performed on a Bruker TimsTOF flex MS system (Bruker Daltonics, Bremen, Germany) equipped with a 10 kHz smartbeam 3D laser. The laser power was fixed at 70 % throughout the experiment. Mass spectra were acquired in positive mode. Mass spectral data were acquired over the mass range of $m/z$ 50–1300 Da. Tissue imaging was performed at a spatial resolution of 50 μm with spectrum comprising 400 laser shots. The signal intensity was normalized to the Root Mean Square for MALDI mass spectra. MS/MS fragmentations performed on the timsTOF flex MS system in the MS/MS mode were used for further detailed structural confirmation of the identified metabolites.

### 2.6. Statistical analysis

Statistical analyses were conducted using SPSS software (version 25.0; International Business Machines Corp., United States). Calculations of normally distributed data were reported as means and standard deviations. Among multiple groups with homogeneous variance, analysis of variance (ANOVA) was used, followed by the least significant difference (LSD) *t*-test; otherwise, Welch's *t*-test and Dunnett's T3 test were adopted. Statistical data with a non-normal distribution were calculated as median (interquartile range) (M [P25, P75]). The chi-square test was used to compare count data among groups. Statistical significance was set at $P < 0.05$.

For non-targeted metabolomics, principal component analysis (PCA) and partial least squares-discriminant analysis (PLS-DA) were applied using SIMCA version 15.0.2 (Umetrics AB, Umea, Sweden). For spatial metabolomic analysis, PCA and orthogonal partial least squares-discriminant analysis (OPLS-DA) were performed using the R stats package (3.5.1) and MetaboAnalystR package(1.0.1). Principal component analysis (PCA) is a technique for dimensionality reduction that identifies a set of orthogonal axes, called principal components, that capture the maximum variance in the data. Partial least squares discriminant analysis (PLS-DA) is a multivariate statistical analysis method used for discriminant analysis. Discriminant analysis is a commonly used statistical analysis method to determine how to classify research objects based on the observed or measured values of several variables. Orthogonal partial least squares discriminant analysis (OPLS-DA) was introduced as an improvement of the PLS-DA approach to discriminate two or more groups (classes) using multivariate data. Specific metabolic markers were screened based on multivariate (O)PLS-DA modeling using t-tests combined with false discovery rate (FDR) correction analysis ($P < 0.05$, FDR$<0.05$).

One-dimensional analyses were performed using a paired Student's t-test to determine P values. A *t*-test was used in conjunction with the PLS-DA method to assess the differences in metabolites between groups (VIP$>1$ and $P < 0.05$).

The diagnostic performance of differential metabolites was assessed using receiver operating characteristic curves (ROC). Diagnostic accuracy was measured using the area under the curve (AUC). We weighed and summarized the sensitivity and specificity of each variable. In terms of AUC, it represented the accuracy of the predictive model, where 1 was denoted 100 % sensitivity and specificity, indicating perfect assignment, whereas an AUC of 0.5 indicated an unreliable test (grey line).

## 3. Results

### 3.1. Population and clinical characteristics

The characteristics of the study population are presented in Table 1. The number of patients with AKI induced by sepsis, surgery (cardiac surgery, renal transplantation, abdominal aortic aneurysm surgery, etc.) and drugs (insecticides, contrast agents, anticancer drugs, etc.) were 6, 23 and 14, respectively. Three cases of post-renal acute kidney injury (kidney stones, bladder cancer, etc.) were also included. There were no significant differences in sex or age between the patient groups. But statistically significant differences were observed among the HC, CKD, and AKI groups across all laboratory indicators ($P < 0.001$). Through pairwise comparison and analysis, we found that patients diagnosed with AKI had significant changes in serum urea, creatinine, uric acid, cystatin C, eGFR, C1q, and NGAL levels compared with both the HC and CKD groups. Although we performed metabolomic analysis on only one serum sample from each patient, serial renal function testing experiments in patients diagnosed with AKI confirmed that the effects on renal function lasted for several days.

### 3.2. Multivariate statistical analysis of metabolites in serum

PCA revealed that QC samples clustered well in both positive and negative ion scan modes (Fig. 1A–B), indicating that the

**Table 1**
Demographic characteristics and laboratory measurements of the studied subjects.

| | HC (n = 38) | CKD (n = 65) | AKI (n = 46) | F/$\chi^2$ | P value |
|---|---|---|---|---|---|
| Demographic characteristics | | | | | |
| Male (n, %) | 21, 55 % | 38, 58 % | 27, 59 % | | |
| Female (n, %) | 17, 45 % | 27, 42 % | 19, 41 % | | |
| Age (years) | 56.3 ± 8.2 | 54.9 ± 12.3 | 59.2 ± 15.0 | | |
| **Laboratory measurements** | | | | | |
| Urea (mmol/L) | 5.04 ± 1.06 | 7.66 (5.82, 13.54)[a] | 20.65 ± 11.10[a,b] | 74.94 | <0.001 |
| Cr (μmol/L) | 67.45 ± 13.85 | 131.85 (104.98, 200.35)[a] | 229.7 (122.40, 368.80)[a,b] | 78.62 | <0.001 |
| UA (μmol/L) | 326.45 ± 60.25 | 432.45 ± 114.68[a] | 490.03 ± 211.97[a,b] | 13.86 | <0.001 |
| CysC (mg/L) | 0.91 ± 0.13 | 2.16 ± 1.16[a] | 2.93 ± 1.45[a,b] | 33.82 | <0.001 |
| eGFR [mL/(min. 1.73m$^2$)] | 87.43 ± 11.94 | 47.15 (29.20, 58.20)[a] | 35.46 ± 18.01[a,b] | 76.73 | <0.001 |
| C1q (mg/L) | 204.37 ± 39.10 | 190.57 ± 40.97 | 140.26 ± 55.70[a,b] | 22.59 | <0.001 |
| NGAL (μg/L) | 104.71 ± 60.81 | 140.05 (107.50, 205.00)[a] | 463.70 (264.63, 1037.10)[a,b] | 66.13 | <0.001 |

HC: group of healthy controls; CKD: group of chronic kidney disease; AKI: group of acute kidney injury. Urea: serum urea; Cr: serum creatinine; UA: serum uric acid; CysC: serum cystatin C; eGFR: estimate the glomerular filtration rate; C1q: serum complement component 1q; NGAL: neutrophil gelatinase-associated lipocalin.

[a] Compared with HC group, $P < 0.05$.

[b] Compared with CKD group, $P < 0.05$.

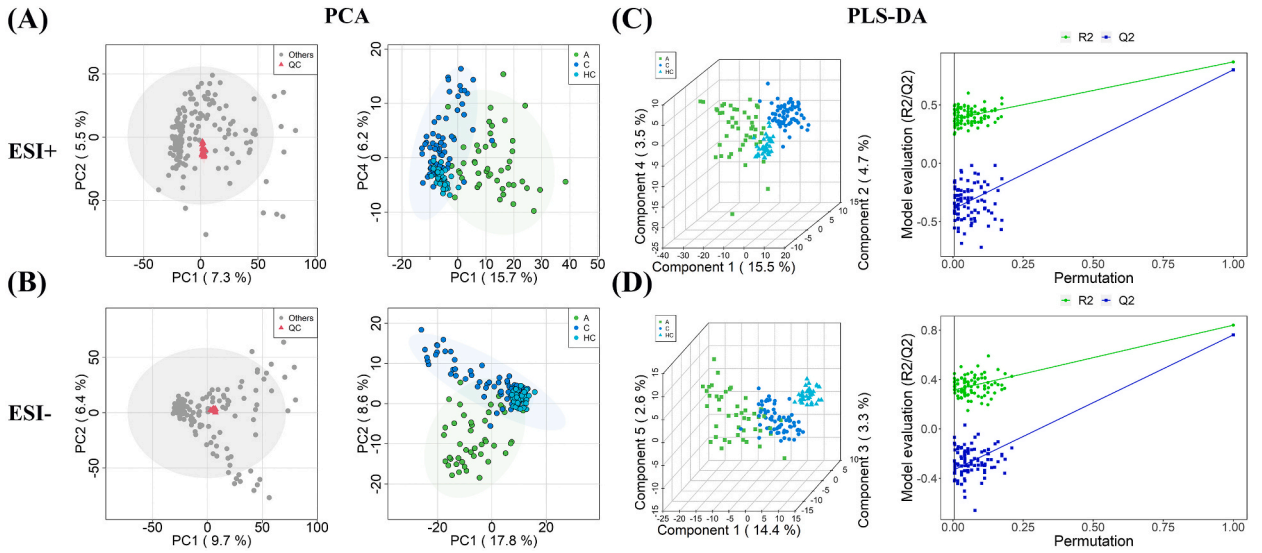


**Fig. 1.** PCA score plots of QC samples and AKI, CKD and HC comparisons (A, B) and PLS-DA score plots with permutation testing of AKI, CKD and HC comparisons (C, D) in the ESI+ and ESI− scan modes.

metabolomics datasets were stable and repeatable. The positive ion mode revealed no distinct classification between the CKD and HC groups (Fig. 1A–B), thus we then applied PLS-DA to obtain an in-depth understanding of the different metabolic profiles with better discriminative power than PCA. The results revealed that both positive and negative modes of metabolite separation were evident in the samples from the three groups (Fig. 1C–D). A random permutation of 200 was performed to determine whether the PLS-DA models were overfitted. PLS-DA demonstrated reliability with positive and negative Q2 distributions and Y-intercepts lower than zero (Fig. 1C–D).

### *3.3. Differential metabolite analysis and identification of serum samples*

Qualitative identification was conducted using publicly available and integrated databases, and 909 and 760 metabolites were identified using positive and negative ion modes, respectively. Subsequently, 365, 275, and 385 different metabolites in the AKI vs. HC, CKD vs. HC, and AKI vs. CKD comparisons were selected using a fold-change threshold >1.5 or <2/3, VIP >1, and a Student's t-test threshold of $P < 0.05$, respectively. Heat maps of 25 representative differential metabolites showed clear clustering among the AKI, CKD, and HC groups in both positive and negative modes (Fig. 2A–B), consistent with the PLS-DA results.

As shown in Table 2, the most abundant classes of metabolites were amino acids, carnitines, and lipids for the AKI vs. HC and CKD vs. HC comparisons, and for the AKI vs. CKD comparison, the most abundant classes were amino acids, carnitines, fatty acids, and lipids. Compared with the HC group, the levels of most amino acids and carnitines in the AKI and CKD groups increased. Additionally, carnitine and free fatty acid levels in the AKI group were significantly higher than those in the CKD group (Fig. 3). Moreover, the

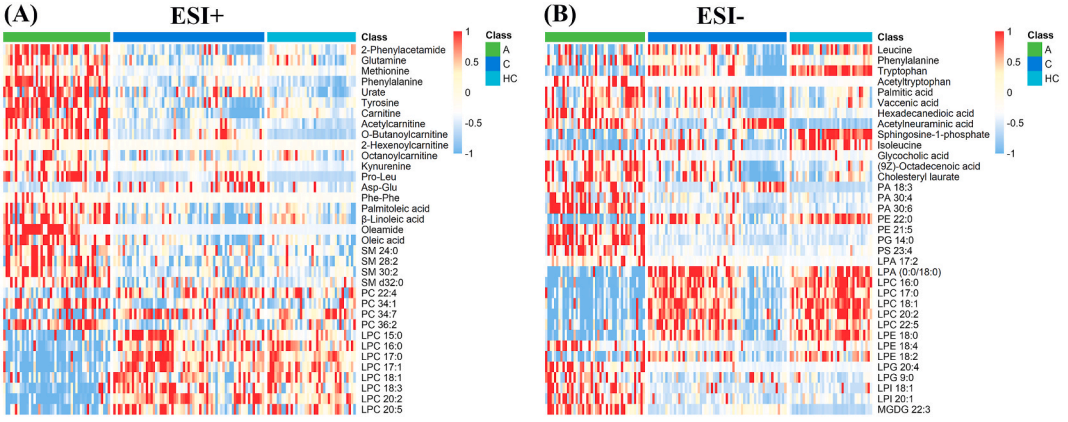


**Fig. 2.** Differential metabolite heat maps in ESI+ (A) and ESI− (B) scan modes. The columns represent samples, the rows represent metabolites, and the relative content of the metabolites is displayed by color.

**Table 2**
List of significantly differential metabolites between AKI vs. HC, CKD vs. HC and AKI vs. CKD comparisons.

| Comparisons | Metabolites | Scan Mode | FC | log 2(FC) | P (T test) | VIP | *m/z* | rt | Adducts |
|---|---|---|---|---|---|---|---|---|---|
| AKI vs. HC | | | | | | | | | |
| Amino acids | Phenylalanine | ESI+ | 1.99 | 1.00 | 2.73E-10 | 1.56 | 166.09 | 258.18 | M + H |
| | Tyrosine | ESI+ | 1.55 | 0.63 | 0.0000041 | 1.28 | 182.08 | 156.01 | M + H |
| | Tryptophan | ESI- | 0.46 | −1.12 | 1.14E-17 | 1.84 | 203.08 | 277.27 | M-H |
| | Isoleucine | ESI- | 0.22 | −2.18 | 1.48E-10 | 1.64 | 392.29 | 435.01 | 3M-H |
| | Kynurenine | ESI+ | 4.40 | 2.14 | 0.00052862 | 1.05 | 209.09 | 256.68 | M + H |
| | Phenylacetylglutamine | ESI+ | 9.63 | 3.27 | 0.000000506 | 1.26 | 265.12 | 301.39 | M + H |
| Carnitines | Carnitine | ESI+ | 1.50 | 0.59 | 0.0000291 | 1.06 | 162.11 | 57.53 | M + H |
| | AcetylCarnitine | ESI+ | 4.19 | 2.07 | 3.57E-09 | 1.50 | 204.12 | 91.72 | M + H |
| Fatty acids | Palmitoleic acid | ESI+ | 1.87 | 0.90 | 0.0000159 | 1.13 | 255.23 | 702.82 | M + H |
| | Oleamide | ESI+ | 43.56 | 5.44 | 3.32E-07 | 1.51 | 282.28 | 731.57 | M + H |
| | Oleic acid | ESI+ | 1.59 | 0.67 | 0.00000109 | 1.30 | 283.26 | 812.69 | M + H |
| **CKD vs. HC** | | | | | | | | | |
| Amino acids | Citrulline | ESI+ | 1.69 | 0.76 | 0.0000289 | 1.40 | 176.10 | 57.97 | M + H |
| | Tryptophan | ESI- | 0.64 | −0.65 | 2.29E-10 | 1.27 | 203.08 | 277.27 | M-H |
| | Kynurenine | ESI+ | 2.00 | 1.00 | 1.75E-12 | 2.19 | 209.09 | 256.68 | M + H |
| | 5-Hydroxytryptophan | ESI- | 7.16 | 2.84 | 0.000000537 | 1.15 | 439.16 | 333.54 | 2M-H |
| | Acetylvaline | ESI- | 0.53 | −0.92 | 0.00030639 | 1.32 | 158.08 | 311.20 | M-H |
| | Acetylaspartate | ESI- | 1.54 | 0.62 | 0.0000755 | 1.03 | 174.04 | 77.02 | M-H |
| | Nicotinuric acid | ESI+ | 10.46 | 3.39 | 0.00029651 | 1.53 | 181.06 | 291.30 | M + H |
| | Asp-glu | ESI+ | 2.20 | 1.14 | 0.0004456 | 1.11 | 263.09 | 385.05 | M + H |
| | Phenylacetyl-L-glutamine | ESI+ | 11.35 | 3.50 | 0.0000132 | 1.54 | 265.12 | 301.39 | M + H |
| | Hydroxyprolyl-Isoleucine | ESI- | 3.74 | 1.90 | 0.00000312 | 1.03 | 243.13 | 310.92 | M-H |
| Carnitines | Butanoylcarnitine | ESI+ | 3.68 | 1.88 | 0.000000998 | 1.47 | 232.15 | 269.51 | M + H |
| | AcetylCarnitine | ESI+ | 1.53 | 0.61 | 0.00047839 | 1.22 | 204.12 | 91.72 | M + H |
| | 2-Hexenoylcarnitine | ESI+ | 2.76 | 1.47 | 0.00000733 | 1.44 | 258.17 | 298.59 | M + H |
| | 2-Octenoylcarnitine | ESI+ | 1.52 | 0.60 | 0.0018023 | 1.01 | 286.20 | 330.64 | M + H |
| **AKI vs. CKD** | | | | | | | | | |
| Amino acids | Methionine | ESI+ | 2.27 | 1.18 | 0.00042235 | 1.10 | 150.06 | 77.84 | M + H |
| | Phenylalanine | ESI+ | 1.67 | 0.74 | 7.67E-08 | 1.51 | 166.09 | 258.18 | M + H |
| | Tyrosine | ESI+ | 1.78 | 0.83 | 7.89E-08 | 1.47 | 182.08 | 156.01 | M + H |
| | Isoleucine | ESI- | 0.30 | −1.75 | 0.00011619 | 1.07 | 392.29 | 408.79 | 3M-H |
| | Acetyltryptophan | ESI- | 22.55 | 4.50 | 0.0001456 | 1.38 | 245.09 | 329.58 | M-H |
| | 5-Hydroxytryptophan | ESI- | 0.34 | −1.56 | 0.0000524 | 1.22 | 439.16 | 317.41 | 2M-H |
| Carnitines | Carnitine | ESI+ | 2.15 | 1.10 | 1.62E-09 | 1.70 | 162.11 | 57.53 | M + H |
| | Acetylcarnitine | ESI+ | 2.48 | 1.31 | 0.000000333 | 1.42 | 204.12 | 77.91 | M + H |
| | Hexanoylcarnitine | ESI+ | 3.49 | 1.80 | 0.000000911 | 1.45 | 260.18 | 314.17 | M + H |
| | Octanoylcarnitine | ESI+ | 1.79 | 0.84 | 0.0014128 | 1.20 | 288.22 | 344.58 | M + H |
| Fatty acids | Palmitoleic acid | ESI+ | 2.15 | 1.10 | 0.00000111 | 1.42 | 255.23 | 702.82 | M + H |
| | Hypogeic acid | ESI- | 1.59 | 0.67 | 0.0018542 | 1.10 | 253.22 | 701.11 | M-H |
| | Oleic acid | ESI+ | 1.75 | 0.81 | 6.08E-08 | 1.50 | 283.26 | 812.69 | M + H |
| | Oleamide | ESI+ | 46.48 | 5.54 | 0.000000326 | 1.69 | 282.28 | 731.57 | M + H |
| | β-Linoleic acid | ESI+ | 1.71 | 0.77 | 0.00000102 | 1.36 | 281.25 | 732.03 | M + H |

FC: fold change; VIP: variable important in projection; *m/z*, mass-to-charge ratio.

lipoylcholine (PC), phosphatidylserine (PS), lysophosphatidylcholine (LPC), lysophosphatidylethanolamine (LPE), and sphingomyelin (SM) classes were metabolically abnormal in the nephrotic population (AKI and CKD groups) compared to the normal population, with most LPC levels significantly decreased (Supplementary Fig.S1). We further performed ROC analysis of each metabolite to determine the diagnostic performance between AKI vs. HC, CKD vs. HC, and AKI vs. CKD. The results showed that 9 metabolites (acetylcarnitine, isoleucine, phenylalanine, kynurenine, trptophan, oleamide, oleic acid, phenylacetylglutamine, sphingosine-1-phosphate) could discriminate AKI from HC (AUC>0.80), 7 metabolites (5-hydroxytryptophan, kynurenine, trptophan, nicotinuric acid, butanoylcarnitine, phenylacetylglutamine, sphingosine-1-phosphate) could discriminate CKD from HC (AUC>0.80), and 8 metabolites (carnitine, acetylcarnitine, hexanoylcarnitine, phenylalanine, tyrosine, methionine, oleamide, oleic acid) could discriminate AKI from CKD (AUC>0.8) (Fig. 3 and Supplementary Table S1). In addition, creatinine has a better diagnostic performance (AUC>0.95) in renal injury (including AKI and CKD) compared with healthy population, but its diagnostic performance in distinguishing AKI from CKD is not deal (AUC = 0.66) (Supplementary Table S1). The results suggest that the differential metabolites we found in the AKI vs. CKD group are expected to be potential biomarkers for distinguishing AKI from CKD. In order to achieve a better diagnostic effect, we selected the differential metabolites with AUC>0.85 for joint diagnostic analysis (Supplementary Fig.S2). It was found that in the AKI vs. HC, CKD vs. HC, and AKI vs. CKD groups, all the AUCs of the combination of two indicators was significantly higher than the AUCs diagnosed by each single indicator, suggesting that the combined diagnosis was superior to the separate diagnosis. And more importantly, in the AKI vs. HC group, the combined diagnosis of phenylalanine and any one of the other four indicators (acetylcarnitine, oleamide, phenylacetylglutamine, and trptophan) had higher AUCs than that of creatinine alone, suggesting that combined biomarkers may be superior to creatinine in the diagnosis of AKI. However, in the CKD vs. HC group, even the diagnostic performance of the combination of three or four indicators was not as good as that of the traditional indicator creatinine in the

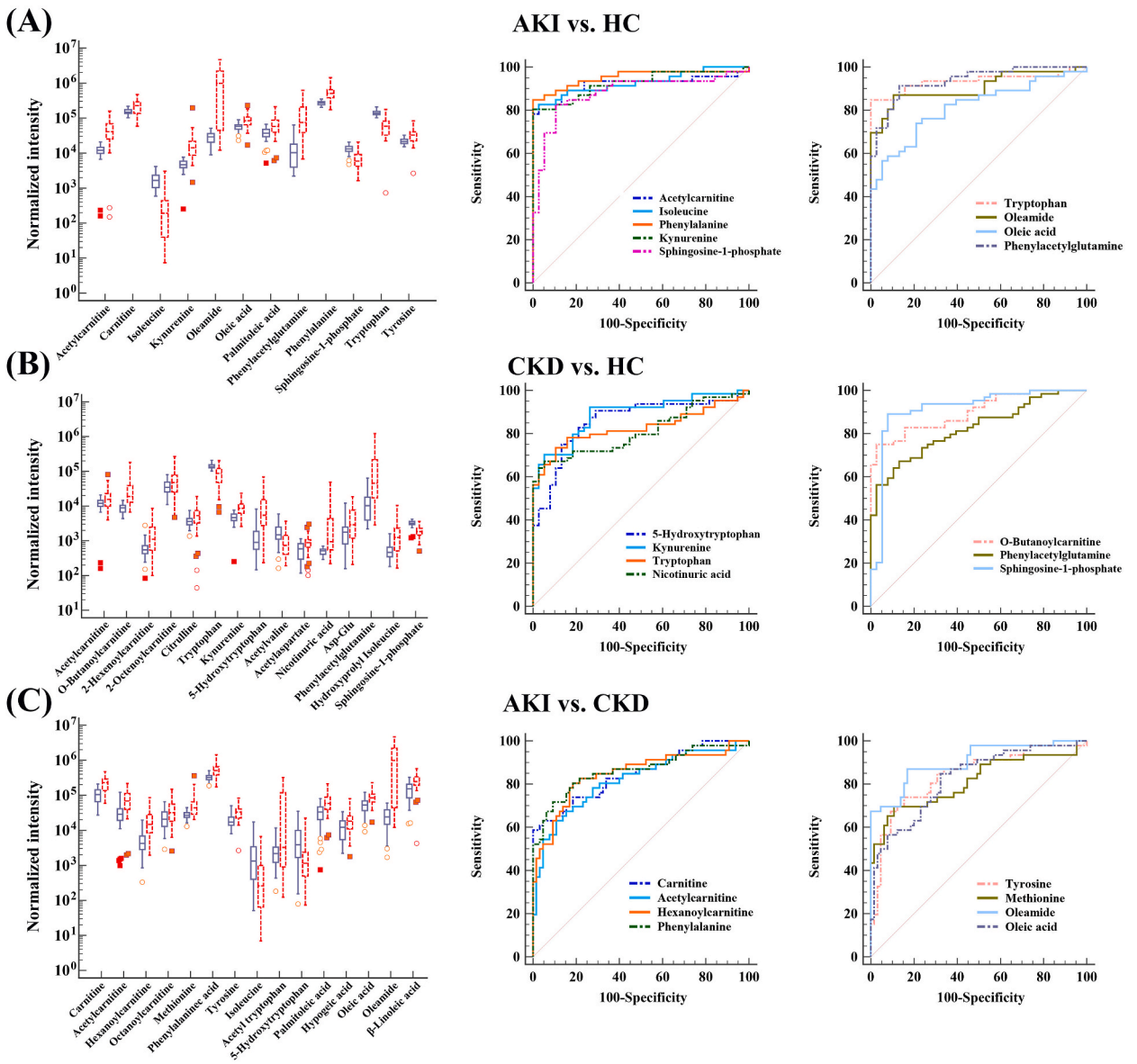


**Fig. 3.** Box plots of normalized intensities and receiver operating characteristic analysis of significantly changed metabolites in AKI vs. HC (A), CKD vs. HC (B) and AKI vs. CKD (C) comparisons.

**Table 3**
List of significantly altered metabolic pathways between AKI vs. HC, CKD vs. HC and AKI vs. CKD comparisons.

| Comparisons | Pathway name | KEGG.id | -log(P) | Impact | Hits |
|---|---|---|---|---|---|
| **AKI vs. HC** | Glycerophospholipid metabolism | hsa00564 | 7.13 | 0.49 | 9 |
| | Tryptophan metabolism | hsa00380 | 1.03 | 0.28 | 4 |
| | Phenylalanine metabolism | hsa 00360 | 0.63 | 0.24 | 1 |
| | Glycerolipid metabolism | hsa00561 | 2.23 | 0.22 | 3 |
| **CKD vs. HC** | Glycerophospholipid metabolism | hsa00564 | 2.66 | 0.31 | 6 |
| | Tryptophan metabolism | hsa00380 | 2.15 | 0.41 | 6 |
| | Glycerolipid metabolism | hsa00561 | 1.97 | 0.22 | 3 |
| | Arginine biosynthesis | hsa 00220 | 0.35 | 0.23 | 1 |
| **AKI vs. CKD** | Glycerophospholipid metabolism | hsa00564 | 5.6994 | 0.48526 | 8 |
| | Linoleic acid metabolism | hsa 00591 | 3.089 | 1 | 2 |
| | Glycerolipid metabolism | hsa00561 | 2.25 | 0.22274 | 3 |
| | Ether lipid metabolism | hsa 00565 | 1.7466 | 0.22892 | 3 |

diagnosis of CKD, indicating creatinine remains a very important indicator of renal function for the diagnosis of chronic kidney injury.

### 3.4. Perturbed pathways analysis of serum samples

An enrichment analysis of the metabolic pathways associated with the differential metabolites was performed (Table 3 and Fig. 4). The results showed that, compared with HC individuals, the differential metabolites were mainly enriched in glycerophospholipid metabolism, tryptophan metabolism, phenylalanine metabolism, and glycerolipid metabolism pathways in the AKI group, and glycerophospholipid metabolism, tryptophan metabolism, glycerolipid metabolism, and arginine biosynthesis pathways in the CKD group. Enriched metabolic pathways of glycerophospholipid, linoleic acid, glycerolipid, and ether lipid metabolism were identified in the AKI vs. CKD comparison.

### 3.5. Spatial metabolomics analysis of kidney of AKI mice

The PCA and OPLS-DA results (Fig. 5A-B) suggested that the NC and AKI groups were significantly different. Next, we performed a one-way *t*-test analysis based on the fold change of metabolites in both groups and obtained 135 metabolites with p-values $<0.05$ (FDR $<0.1$) and VIP $>1$, of which 71 decreased and 64 increased, as shown in the volcano plot (Fig. 5C). The heat map showed that the two groups differed in the metabolic abundance of amino acids and lipid metabolites (Fig. 5D). The differential metabolite pathway enrichment analysis (Fig. 5E) showed that the metabolic pathways significantly interfered in the AKI group were mainly oxytocin signaling pathway, platelet activation, ferroptosis, aldosterone synthesis and secretion and purine metabolism.

H&E staining revealed that the tubular lumen narrowed and atrophied, the glomerulus atrophied, the cortical labyrinth tubule arrangement was disturbed, the tubular gap widened in the AKI group. Renal function index showed a significant increase in creatinine and urea nitrogen levels (Fig. 6), suggesting that the AKI mouse model was successfully established. Next, kidney tissues from AKI and normal mice were examined using MALDI-TOF MS analysis. We detected significant differences in the abundance of various metabolites, such as amino acids, carnitine, organic acids, fatty acids, and lipids, in situ (Fig. 6). The findings showed that Most differentially expressed amino acid-like metabolites were distributed in the cortical region. In the kidneys of mice with AKI, carnitine metabolites were significantly upregulated in the cortex and downregulated in the medulla. Differential small-molecule organic acids mainly accumulated in the inner cortex with increased levels in the AKI group, whereas fatty acids were mainly distributed in the outer cortex with decreased levels. Lipids were either upregulated or downregulated in the cortex and medulla of AKI mouse kidneys These results suggest tissue heterogeneity in the distribution of differential metabolites in AKI kidneys.

## 4. Discussion

Acute kidney injury (AKI) is a relatively common critical clinical illness; however, no effective diagnostic tool or treatment is available. Metabolomics best reflects disease molecular phenotypes, as it directly reflects the underlying biochemical activity of cells/tissues and enables us to understand the pathophysiological mechanisms underlying AKI from a metabolic perspective to provide potential therapeutic and/or differential diagnostic biomarkers.

We analyzed 46 AKI cases, 65 CKD cases, and 38 serum samples from age- and sex-matched healthy donors via mass spectrometric analysis (LC-MS/MS). The AKI and CKD groups exhibited significant alterations in amino acid, carnitine, and lipid levels compared with the healthy control group, indicating that kidney injury might lead to dysregulated metabolic pathways of amino acids, fatty acids, and lipids. Moreover, pidemiological and etiological studies have indicated that acute kidney injury (AKI) is closely correlated with chronic kidney disease (CKD), and CKD is a risk factor for AKI; in turn, AKI patients have an increased risk of developing CKD [26]. In this study, we also compared the metabolic differences between AKI and CKD groups for the first time and found that the two groups had different amino acid, carnitine, and fatty acid levels. This implies that these two diseases have different metabolic and

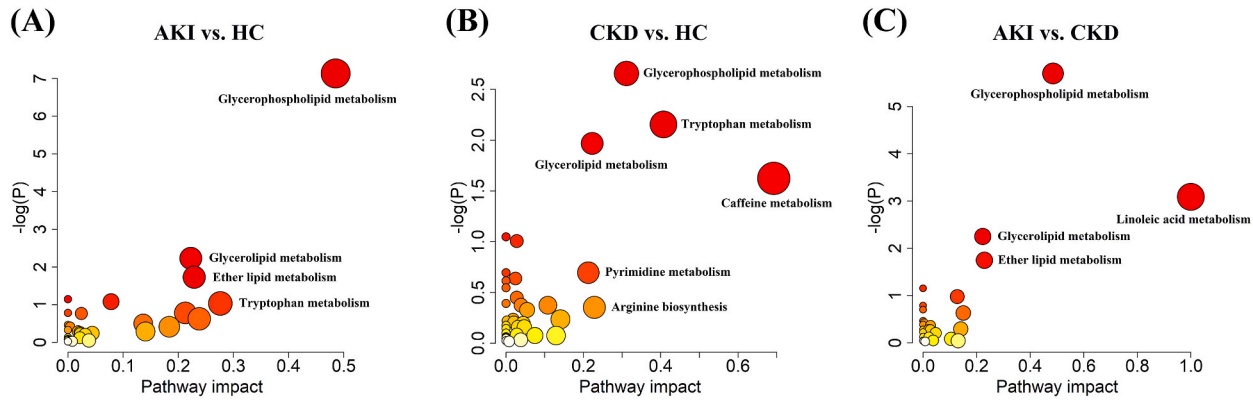


**Fig. 4.** Bubble diagram of metabolic pathways in AKI vs. HC (A), CKD vs. HC (B) and AKI vs. CKD (C) comparisons.

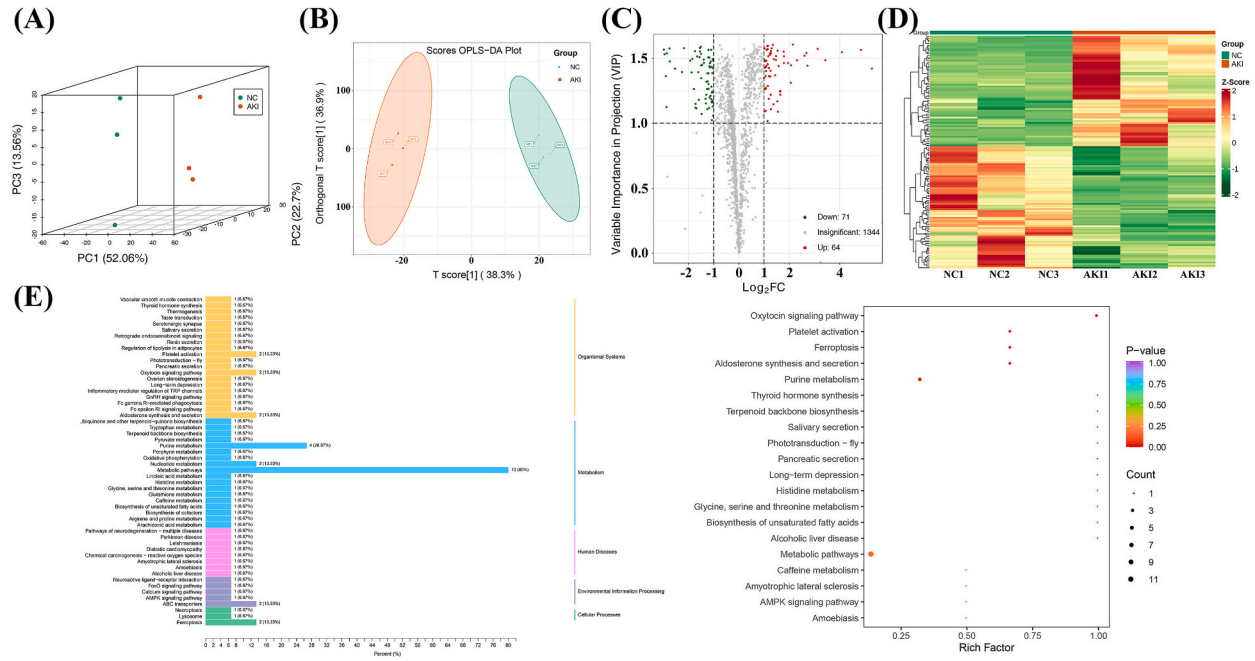


**Fig. 5.** The PCA score plot (A), OPLS-DA score plot (B), volcano plot (C), heat map (D) and pathway enrichment analysis (E) of differential metabolites in AKI mouse model and negative control in spatial metabolomics analysis.

pathophysiological mechanisms.

Amino acid metabolism is inextricably linked to kidneys. The kidney maintains a balanced amino acid metabolism by synthesizing, degrading, filtering, reabsorbing, and urinating amino acids [27]. Human CKD renal biopsy and post-ischemia/reperfusion (I/R) injury transcript maps of mice indicate dysregulated amino acid metabolism [28]. We also found that patients in the AKI and CKD groups had elevated serum amino acid levels (except tryptophan). It has been previously reported that an increase in amino acid excretion is a potential marker of kidney dysfunction [29]. In the case of kidney dysfunction, the defense and repair processes significantly increase the amino acids required for protein synthesis, which may be one of the reasons why the amino acid levels decrease in kidney tissue but increase in serum [29]. Multiple studies have indicated that tryptophan concentration is closely related to AKI severity. For instance, patients with liver cirrhosis and AKI have activated tryptophan-kynurenine and transsulfuration pathways. It has been proven that the downstream product of the kynurenine pathway, quinolinic acid, is correlated with the risk of AKI in experimental models and in patients with severe symptoms [30,31]. Furthermore, a metabolomic study reported that some novel biomarkers, such as acylcarnitine and tryptophan metabolites, performed better than creatinine in a stratified CKD analysis [32]. Our study revealed that tryptophan-kynurenine metabolism was aberrantly activated in the AKI and CKD groups, which is consistent with previous studies. Notably, phenylacetylglutamine (PAGln) levels were elevated in both groups. PAGln is a novel gut flora metabolic derivative associated with cardiovascular diseases [33]. This implies a possible connection between the gut flora and kidney injury. PAGln enhances platelet activation-related phenotypes and thrombosis. Therefore, patients with AKI and CKD should be aware of the occurrence of cardiovascular diseases and major adverse cardiac events (myocardial infarction, stroke, or death).

Carnitine plays a significant role in the oxidative metabolism of fatty acids and branched-chain amino acids. Fatty acids can supply energy via oxidation of the mitochondrial membrane in the form of acylcarnitine by binding to carnitine [34]. During acute kidney injury, the expression and activity of mitochondrial and peroxisomal fatty acid oxidation enzymes in renal tissue are significantly reduced, and fatty acid oxidation is dysregulated [19]. In this study, we observed that the AKI and CKD groups had elevated serum levels of L-carnitine, acetylcarnitine, and other short-chain acylcarnitines compared to the normal control group. It was previously reported that rats have increased free carnitine and short-chain acylcarnitine levels in the serum 48 h after renal I/R injury [30]. This finding is consistent with our results; therefore, we speculate that mitochondrial damage occurs in renal injury. On the other hand, some researchers have suggested that L-carnitine, acetylcarnitine, and other short-chain acylcarnitines are conducive to various diseases (including renal diseases) by increasing mitochondrial carnitine concentration and stimulating the Krebs cycle [30]. Thus, elevated carnitine levels may be a protective response of tissues to injuries.

Disorders in lipid metabolism are another feature of kidney injury. Injury to cholesterol metabolism, increased fat intake or synthesis, increased fatty acid oxidation, lipid droplet accumulation, and bioactive sphingomyelin imbalance (e.g., ceramide, ceramide-1-phosphate, and sphingosine 1-phosphate (S1P)) all lead to renal diseases [35]. Aberrant lipid metabolism leads to an increased production of reactive oxygen species (ROS), oxidative stress, inflammation, and cell death. Correspondingly, we demonstrated aberrant metabolism of PC, PS, LPC, LPE, and SM in the AKI and CKD groups. Serum LPC levels were significantly reduced. One possible explanation is a reduction in the activity of lecithin cholesterol acyltransferase (an enzyme that converts unesterified

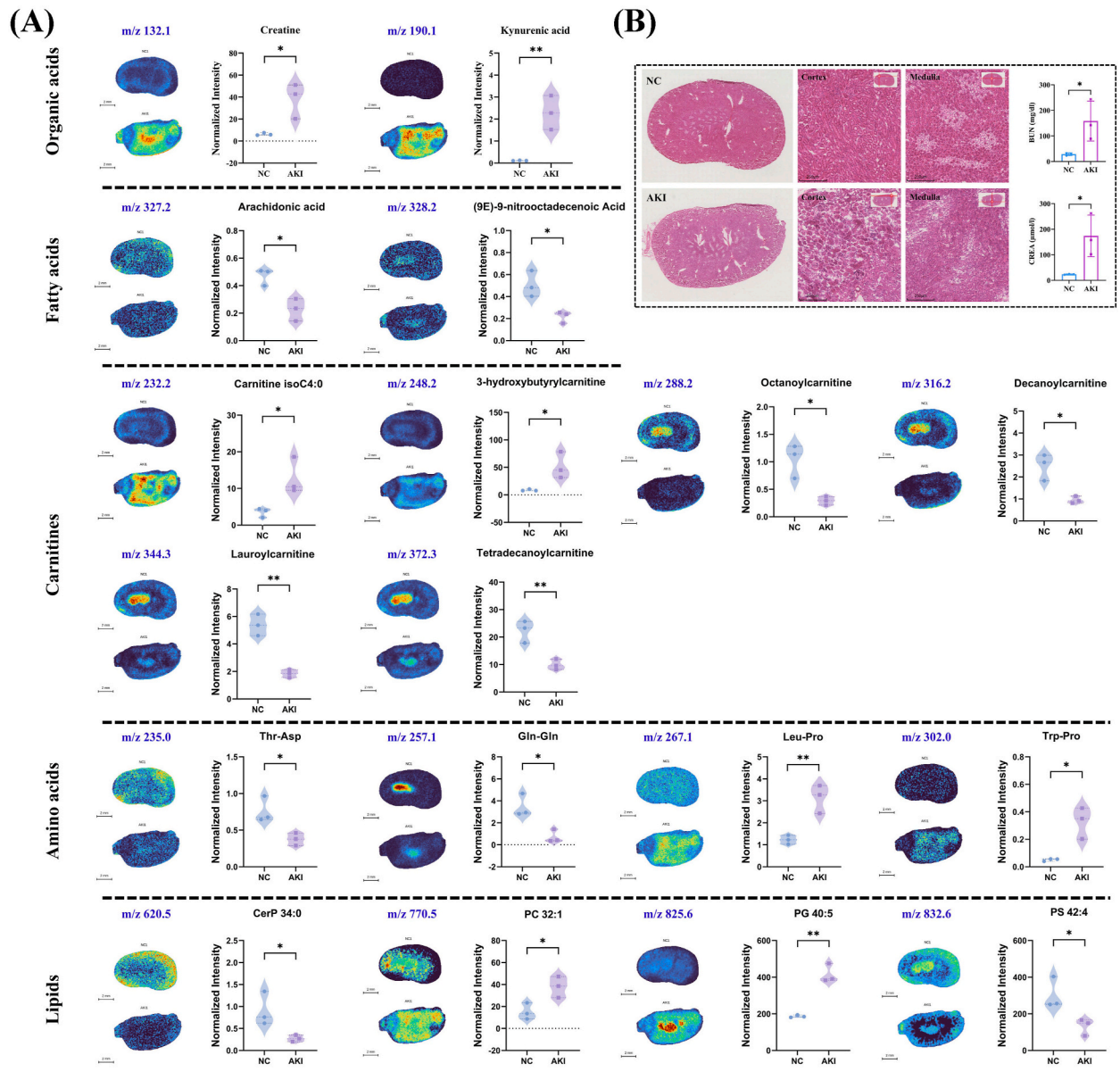


**Fig. 6.** In situ mass spectrometry imaging with normalized intensities of various metabolites (A) and H&E staining (B) in kidney tissues between AKI mouse model and negative control in spatial metabolomics analysis. *P* < 0.05; P* < 0.01.*

cholesterol and phosphatidylcholine to esterified cholesterol and lysophosphatidylcholine) [19]. Additionally, S1P levels were lower in the AKI and CKD groups than in the normal group. S1P is a sphingosine-signaling lipid derived from sphingosine via the action of sphingosine kinase. S1P is conducive to the trafficking and effector functions of lymphocytes and hematopoietic cells, and can protect against tissue injury in various forms [36]. Increasing S1P levels in circulation can alleviate lung injuries that occur during ex vivo perfusion [37], and exogenous S1P has protective effects on liver and kidney injuries due to hepatic I/R injury [38]. The S1P signaling pathway in perivascular cells plays a critical role in renal fibrosis [39], indicating that more attention should be paid to S1P levels during kidney injury. Furthermore, the S1P metabolic pathway may be a target for improving renal fibrosis in acute or chronic renal diseases.

The metabolic differences between the AKI and CKD groups were analyzed to illustrate their distinct metabolic mechanisms. We found that the AKI group had significantly upregulated carnitine and free fatty acid levels compared to the CKD group, indicating that the AKI group had a more severe fatty acid metabolism disorder. Studies have consistently shown that AKI is associated with mitochondrial dysfunction and ATP depletion. Fatty acid oxidation is a favorable energy source for the kidney, and the suppression of fatty acid oxidation is one of the major pathophysiological alterations in AKI [40,41]. Key genes regulating fatty acid oxidation, such as CPT1 and medium-chain-specific acyl-CoA dehydrogenase, are downregulated in AKI induced by I/R and cisplatin, leading to reduced

utilization of fatty acids by tubular endothelial cells (TECs) [42]. Another study reported that impaired fatty acid beta-oxidation aggravated renal fibrosis, and fatty acid beta-oxidation repair arrested the progression of renal disease. Hence, AKI-related kidney injuries can be ameliorated by reinforcing fatty acid beta-oxidation. Moreover, eight significant differential metabolites, carnitine, acetylcarnitine, hexanoylcarnitine, phenylalanine, tyrosine, methionine, oleamide, and oleic acid, showed good diagnostic performance (all AUC>0.8) in discriminating AKI from CKD. Most of these are related to fatty acid metabolism and may be considered reliable indicators for the diagnosis of AKI.

From the limited clinical evidence, AKI induced by transcatheter aortic valve replacement, kidney transplantation and coronary artery bypass grafting is mainly related to abnormal metabolism of amino acids (such as 5-adenosylhomocysteine, tryptophan and symmetric dimethylarginine); whereas in patients with vancomycin-associated AKI, oxidative stress is considered a key mechanism of vancomycin-associated renal injury. In addition to abnormalities in amino acid metabolism, the 5-hydroxyindoleacetic acid/5-hydroxytryptophan ratio was identified as a surrogate marker for vancomycin-associated AKI [43]. More, metabolomics-derived findings in experimental AKI showed that ischemia induces multiple deterioration of lipid, glucose, and energy metabolism. Both lipopolysaccharide and cisplatin also impaired lipid, amino acid and energy metabolism. Cisplatin specifically modulates the tryptophan pathway, which is likely to be a key mechanism of cisplatin-induced AKI [44].

Through spatial metabolomics, MS imaging enables the direct visualization of metabolite distributions in tissues, providing insight into disease-associated biochemical changes within specific structures [12]. To obtain better information on the spatial distribution of AKI metabolites, we studied kidney tissues from mice with AKI using MALDI-TOF-MS-based spatially resolved metabolomics. We found significant differences in the abundance of amino acids, carnitine, organic acids, fatty acids, and lipids (consistent with the differential metabolite species screened in clinical patient sera) in the kidneys of healthy and mice with AKI. In addition, we found that amino acid, carnitine, organic acid, and fatty acid metabolites were significantly altered in the kidney cortex of AKI mice, whereas lipid metabolites were differentially distributed in the cortex and medulla of AKI mice. Our study revealed tissue-heterogeneous metabolic reprogramming in AKI, which may provide more comprehensive and detailed information on the molecular pathology of AKI in the kidney tissue.

Overall, our study indicated that patients with AKI and CKD had an aberrant metabolism of amino acids, carnitines, and lipids, which are closely associated with physiological dysfunction in kidney injury. Additionally, we compared the metabolic differences between AKI and CKD patients for the first time, showing that AKI patients had more severe suppression of fatty acid oxidation. Furthermore, spatial metabolomics has revealed metabolic reprogramming with tissue heterogeneity in patients with AKI. Although we provide a new direction for understanding the pathological mechanisms of AKI, this study has some limitations. First, we were unable to identify metabolites associated with the AKI phenotype, and future studies should attempt to determine whether different AKI phenotypes have different metabolomes. Second, the sample size was small, and we hope to conduct a multicenter study with a large sample size in a later stage to reduce sampling error. Third, according to the definitions of metabolite identification as described by Schrimpe-Rutledge [45], all the metabolites determined in this study would be considered as putative identification (Level 2), which lack the reference standard acquisition but used MS/MS data in combination of precursor $m/z$ and retention time to derive the structural information. Thus, these findings need to be validated and the specific mechanisms underlying these metabolic pathways require further elucidation.

## Data availability statement

Data associated with this study has not been deposited into a publicly available repository. Data will be made available on request.

## Ethics approval

The studies involving human participants were reviewed and approved by the Medical Ethics Committee of Mianyang Central Hospital. All enrolled patients signed written informed consent forms. Animal experiments have been approved by the Laboratory Animal Management and Use Committee of Wuhan Servicebio Technology Co., Ltd (No.2021098).

## Funding statement

This work was financially supported by Sichuan Science and Technology Program (Grant No. 2022NSFSC0735) and NHC Key Laboratory of Nuclear Technology Medical Transformation (Mianyang Central Hospital) (Grant No.2022HYX007).

## CRediT authorship contribution statement

**Bei Xu:** Funding acquisition, Writing – original draft. **Wanyi Li:** Writing – original draft. **Yamei Zhang:** Data curation. **Yan Chen:** Data curation. **Jiafu Feng:** Formal analysis, Methodology. **Xiangrong Song:** Writing – review & editing.

## Declaration of competing interest

The authors declare that they have no known competing financial interests or personal relationships that could have appeared to influence the work reported in this paper.

## Acknowledgements

Not applicable.

## Appendix A. Supplementary data

Supplementary data to this article can be found online at https://doi.org/10.1016/j.heliyon.2023.e21171.

## References

[1] C. Ronco, R. Bellomo, J.A. Kellum, Acute kidney injury, Lancet (London, England) 394 (10212) (2019) 1949–1964, https://doi.org/10.1016/S0140-6736(19)32563-2.
[2] O. Rewa, S.M. Bagshaw, Acute kidney injury-epidemiology, outcomes and economics. Nature reviews, Nephrology 10 (4) (2014) 193–207, https://doi.org/10.1038/nrneph.2013.282.
[3] P. Pickkers, M. Darmon, E. Hoste, M. Joannidis, M. Legrand, M. Ostermann, J.R. Prowle, A. Schneider, M. Schetz, Acute kidney injury in the critically ill: an updated review on pathophysiology and management, Intensive Care Med. 47 (8) (2021) 835–850, https://doi.org/10.1007/s00134-021-06454-7.
[4] L. Sykes, R. Nipah, P. Kalra, D. Green, A narrative review of the impact of interventions in acute kidney injury, J. Nephrol. 31 (4) (2018) 523–535, https://doi.org/10.1007/s40620-017-0454-2.
[5] J. Vanmassenhove, J. Kielstein, A. Jörres, W.V. Biesen, Management of patients at risk of acute kidney injury, Lancet (London, England) 389 (10084) (2017) 2139–2151, https://doi.org/10.1016/S0140-6736(17)31329-6.
[6] R.J. DeBerardinis, C.B. Thompson, Cellular metabolism and disease: what do metabolic outliers teach us? Cell 148 (6) (2012) 1132–1144, https://doi.org/10.1016/j.cell.2012.02.032.
[7] T.J. Rabelink, P. Carmeliet, Renal metabolism in 2017: glycolytic adaptation and progression of kidney disease. Nature reviews, Nephrology 14 (2) (2018) 75–76, https://doi.org/10.1038/nrneph.2017.173.
[8] V. Padovano, C. Podrini, A. Boletta, M.J. Caplan, Metabolism and mitochondria in polycystic kidney disease research and therapy. Nature reviews, Nephrology 14 (11) (2018) 678–687, https://doi.org/10.1038/s41581-018-0051-1.
[9] M. Alsahli, J.E. Gerich, Renal glucose metabolism in normal physiological conditions and in diabetes, Diabetes Res. Clin. Pract. 133 (2017) 1–9, https://doi.org/10.1016/j.diabres.2017.07.033.
[10] I. Rowe, M. Chiaravalli, V. Mannella, V. Ulisse, G. Quilici, M. Pema, X.W. Song, H. Xu, S. Mari, F. Qian, Y. Pei, G. Musco, A. Boletta, Defective glucose metabolism in polycystic kidney disease identifies a new therapeutic strategy, Nat. Med. 19 (4) (2013) 488–493, https://doi.org/10.1038/nm.3092.
[11] S. Liu, Y. Gui, M.S. Wang, L. Zhang, T. Xu, Y. Pan, K. Zhang, Y. Yu, L. Xiao, Y. Qiao, C. Bonin, G. Hargis, T. Huan, Y. Yu, J. Tao, R. Zhang, D.L. Kreutzer, Y. Zhou, X.J. Tian, Y. Wang, D. Zhou, Serum integrative omics reveals the landscape of human diabetic kidney disease, Mol. Metabol. 54 (2021), 101367, https://doi.org/10.1016/j.molmet.2021.101367.
[12] Z. Wang, W. Fu, M. Huo, B. He, Y. Liu, L. Tian, W. Li, Z. Zhou, B. Wang, J. Xia, Y. Chen, J. Wei, Z. Abliz, Spatial-resolved metabolomics reveals tissue-specific metabolic reprogramming in diabetic nephropathy by using mass spectrometry imaging, Acta Pharm. Sin. B 11 (11) (2021) 3665–3677, https://doi.org/10.1016/j.apsb.2021.05.013.
[13] Y.L. Feng, G. Cao, D.Q. Chen, N.D. Vaziri, L. Chen, J. Zhang, M. Wang, Y. Guo, Y.Y. Zhao, Microbiome-metabolomics reveals gut microbiota associated with glycine-conjugated metabolites and polyamine metabolism in chronic kidney disease, Cell. Mol. Life Sci.: CMLS 76 (24) (2019) 4961–4978, https://doi.org/10.1007/s00018-019-03155-9.
[14] K. Mercier, S. McRitchie, W. Pathmasiri, A. Novokhatny, R. Koralkar, D. Askenazi, P.D. Brophy, S. Sumner, Preterm neonatal urinary renal developmental and acute kidney injury metabolomic profiling: an exploratory study, Pediatr. Nephrol. 32 (1) (2017) 151–161, https://doi.org/10.1007/s00467-016-3439-9.
[15] T.K. Sigdel, A.W. Schroeder, J.Y.C. Yang, R.D. Sarwal, J.M. Liberto, M.M. Sarwal, Targeted urine metabolomics for monitoring renal allograft injury and immunosuppression in pediatric patients, J. Clin. Med. 9 (8) (2020) 2341, https://doi.org/10.3390/jcm9082341.
[16] B. Tan, J. Chen, S. Qin, C. Liao, Y. Zhang, D. Wang, S. Li, Z. Zhang, P. Zhang, F. Xu, Tryptophan pathway-targeted metabolomics study on the mechanism and intervention of cisplatin-induced acute kidney injury in rats, Chem. Res. Toxicol. 34 (7) (2021) 1759–1768, https://doi.org/10.1021/acs.chemrestox.1c00110.
[17] W. Guo, Y. Wang, Y. Wu, J. Liu, Y. Li, J. Wang, S. Ou, W. Wu, Integration of transcriptomics and metabolomics reveals the molecular mechanisms underlying the effect of nafamostat mesylate on rhabdomyolysis-induced acute kidney injury, Front. Pharmacol. 13 (2022), 931670, https://doi.org/10.3389/fphar.2022.931670.
[18] F. Ping, Y. Li, Y. Cao, J. Shang, Z. Zhang, Z. Yuan, W. Wang, Y. Guo, Metabolomics analysis of the development of sepsis and potential biomarkers of sepsis-induced acute kidney injury, Oxid. Med. Cell. Longev. 2021 (2021), 6628847, https://doi.org/10.1155/2021/6628847.
[19] J. Sun, M. Shannon, Y. Ando, L.K. Schnackenberg, N.A. Khan, D. Portilla, R.D. Beger, Serum metabolomic profiles from patients with acute kidney injury: a pilot study, J. Chromatogr., B: Anal. Technol. Biomed. Life Sci. 893–894 (2012) 107–113, https://doi.org/10.1016/j.jchromb.2012.02.042.
[20] J.T. Kurzhagen, S. Dellepiane, V. Cantaluppi, H. Rabb, AKI: an increasingly recognized risk factor for CKD development and progression, J. Nephrol. 33 (6) (2020) 1171–1187, https://doi.org/10.1007/s40620-020-00793-2.
[21] M. Zdziechowska, A. Gluba-Brzózka, A.R. Poliwczak, B. Franczyk, M. Kidawa, M. Zielinska, J. Rysz, Serum NGAL, KIM-1, IL-18, L-FABP: new biomarkers in the diagnostics of acute kidney injury (AKI) following invasive cardiology procedures, Int. Urol. Nephrol. 52 (11) (2020) 2135–2143, https://doi.org/10.1007/s11255-020-02530-x.
[22] D.J. Oh, A long journey for acute kidney injury biomarkers, Ren. Fail. 42 (1) (2020) 154–165, https://doi.org/10.1080/0886022X.2020.1721300.
[23] Kidney Disease Improving Global Outcomes (Kdigo), Clinical practice guideline for acute kidney injury, Kidney Int. Suppl. 2 (2012) 1–138.
[24] KDIGO 2012 clinical practice guideline for the evaluation and management of chronic kidney disease, Kidney Int. 3 (1) (2013) 5–14.
[25] C. Yan, D. Wu, L. Gan, J. Wang, W. Yang, B. Xu, Significant metabolic alterations in non-small cell lung cancer patients by epidermal growth factor receptor-targeted therapy and PD-1/PD-L1 immunotherapy, Front. Pharmacol. 13 (2022), 949745, https://doi.org/10.3389/fphar.2022.949745.
[26] F. Ginhoux, J.L. Schultze, P.J. Murray, J. Ochando, S.K. Biswas, New insights into the multidimensional concept of macrophage ontogeny, activation and function, Nat. Immunol. 17 (1) (2016) 34–40, https://doi.org/10.1038/ni.3324.
[27] X. Li, S. Zheng, G. Wu, Amino acid metabolism in the kidneys: nutritional and physiological significance, Adv. Exp. Med. Biol. 1265 (2020) 71–95, https://doi.org/10.1007/978-3-030-45328-2_5.
[28] S.E. Piret, Y. Guo, A.A. Attallah, S.J. Horne, A. Zollman, D. Owusu, J. Henein, V.S. Sidorenko, M.P. Revelo, T. Hato, A. Ma'ayan, J.C. He, S.K. Mallipattu, Krüppel-like factor 6-mediated loss of BCAA catabolism contributes to kidney injury in mice and humans, Proc. Natl. Acad. Sci. U.S.A. 118 (23) (2021), e2024414118, https://doi.org/10.1073/pnas.2024414118.
[29] J.L. Izquierdo-Garcia, N. Nin, P. Cardinal-Fernandez, Y. Rojas, M. de Paula, R. Granados, L. Martínez-Caro, J. Ruíz-Cabello, J.A. Lorente, Identification of novel metabolomic biomarkers in an experimental model of septic acute kidney injury, Am. J. Physiol. Ren. Physiol. 316 (1) (2019) F54–F62, https://doi.org/10.1152/ajprenal.00315.2018.

[30] N.V. Andrianova, V.A. Popkov, N.S. Klimenko, A.V. Tyakht, G.V. Baydakova, O.Y. Frolova, L.D. Zorova, I.B. Pevzner, D.B. Zorov, E.Y. Plotnikov, Microbiome-Metabolome Signature of Acute Kidney Injury. Metabolites 10 (4) (2020) 142, https://doi.org/10.3390/metabo10040142.
[31] J.S. Bajaj, G. Garcia-Tsao, K.R. Reddy, J.G. O'Leary, H.E. Vargas, J.C. Lai, P.S. Kamath, P. Tandon, R.M. Subramanian, P. Thuluvath, A. Fagan, T. Sehrawat, R. de la Rosa Rodriguez, L.R. Thacker, F. Wong, Admission urinary and serum metabolites predict renal outcomes in hospitalized patients with cirrhosis, Hepatology (Baltimore, Md 74 (5) (2021) 2699–2713, https://doi.org/10.1002/hep.31907.
[32] B. Hocher, J. Adamski, Metabolomics for clinical use and research in chronic kidney disease. Nature reviews, Nephrology 13 (5) (2017) 269–284, https://doi.org/10.1038/nrneph.2017.30.
[33] I. Nemet, P.P. Saha, N. Gupta, W. Zhu, K.A. Romano, S.M. Skye, T. Cajka, M.L. Mohan, L. Li, Y. Wu, M. Funabashi, A.E. Ramer-Tait, S.V. Naga Prasad, O. Fiehn, F.E. Rey, W.H.W. Tang, M.A. Fischbach, J.A. DiDonato, S.L. Hazen, A cardiovascular disease-linked gut microbial metabolite acts via adrenergic receptors, Cell 180 (5) (2020) 862–877.e22, https://doi.org/10.1016/j.cell.2020.02.016.
[34] N. Longo, M. Frigeni, M. Pasquali, Carnitine transport and fatty acid oxidation, Biochim. Biophys. Acta 1863 (10) (2016) 2422–2435, https://doi.org/10.1016/j.bbamcr.2016.01.023.
[35] A. Mitrofanova, G. Burke, S. Merscher, A. Fornoni, New insights into renal lipid dysmetabolism in diabetic kidney disease, World J. Diabetes 12 (5) (2021) 524–540, https://doi.org/10.4239/wjd.v12.i5.524.
[36] H. Fyrst, J.D. Saba, An update on sphingosine-1-phosphate and other sphingolipid mediators, Nat. Chem. Biol. 6 (7) (2010) 489–497, https://doi.org/10.1038/nchembio.392.
[37] J.H. Mehaffey, E.J. Charles, A.K. Narahari, S. Schubert, V.E. Laubach, N.R. Teman, K.R. Lynch, I.L. Kron, A.K. Sharma, Increasing circulating sphingosine-1-phosphate attenuates lung injury during ex vivo lung perfusion, J. Thorac. Cardiovasc. Surg. 156 (2) (2018) 910–917, https://doi.org/10.1016/j.jtcvs.2018.02.090.
[38] S.W. Park, M. Kim, S.W. Chen, K.M. Brown, V.D. D'Agati, H.T. Lee, Sphinganine-1-phosphate protects kidney and liver after hepatic ischemia and reperfusion in mice through S1P1 receptor activation, Laboratory investigation; a journal of technical methods and pathology 90 (8) (2010) 1209–1224, https://doi.org/10.1038/labinvest.2010.102.
[39] A. Huwiler, J. Pfeilschifter, Sphingolipid signaling in renal fibrosis, Matrix Biol.: journal of the International Society for Matrix Biology 68–69 (2018) 230–247, https://doi.org/10.1016/j.matbio.2018.01.006.
[40] H. Ma, X. Guo, S. Cui, Y. Wu, Y. Zhang, X. Shen, C. Xie, J. Li, Dephosphorylation of AMP-activated protein kinase exacerbates ischemia/reperfusion-induced acute kidney injury via mitochondrial dysfunction, Kidney Int. 101 (2) (2022) 315–330, https://doi.org/10.1016/j.kint.2021.10.028.
[41] Kidney Int. (2019), https://doi.org/10.1016/j.kint.2019.08.019.
[42] Z. Gao, X. Chen, Fatty acid β-oxidation in kidney diseases: perspectives on pathophysiological mechanisms and therapeutic opportunities, Front. Pharmacol. 13 (2022), 805281, https://doi.org/10.3389/fphar.2022.805281.
[43] D. Patschan, S. Patschan, I. Matyukhin, O. Ritter, W. Dammermann, Metabolomics in acute kidney injury: the clinical perspective, J. Clin. Med. 12 (12) (2023) 4083, https://doi.org/10.3390/jcm12124083.
[44] D. Patschan, S. Patschan, I. Matyukhin, M. Hoffmeister, M. Lauxmann, O. Ritter, W. Dammermann, Metabolomics in acute kidney injury: the experimental perspective, J. Clin. Med. Res. 15 (6) (2023) 283–291, https://doi.org/10.14740/jocmr4913.
[45] A.C. Schrimpe-Rutledge, S.G. Codreanu, S.D. Sherrod, J.A. McLean, Untargeted metabolomics strategies-challenges and emerging directions, J. Am. Soc. Mass Spectrom. 27 (12) (2016) 1897–1905, https://doi.org/10.1007/s13361-016-1469-y.